Chemical and mineralogical properties of Guanajibo clay (Plinthic Kandiudults)[1]

*Bianca Pérez-Lizasuain[2], Miguel A. Muñoz[3],
Julia M. O'Hallorans[4] and Wanda I. Lugo[5]*

ABSTRACT

A profile of Guanajibo clay (Plinthic Kandiudults) was evaluated to determine the ironstone content in the horizons and its chemical, physical and mineralogical properties. The mineralogy was characterized by X-ray diffraction (XRD) and the iron and aluminum oxide content determined by selective dissolution, using citrate-bicarbonate dithionite (CBD) and ammonium oxalate (OX) extractions. Soil color and the color of ground ironstone were determined with Munsell color charts. Soil texture, pH, and effective cation exchange capacity (ECEC) were also evaluated. The highest content of ironstone per unit mass was found in the Ap horizon (4.6%), decreasing in the Bt (0.9%) and Btv1 (1.0%) horizons. An increase in ironstone content was observed in the Btv2 horizon (3.8%), which suggests that this horizon was formed from alluvial deposits containing ironstone. No ironstone was found in the Btv3 horizon. The texture of the Ap horizon was a sandy clay, and the other horizons had a clay texture. Clay content reached a maximum value of 92.8% in the Btv3. The ECEC was low for the whole profile, ranging from 2.37 cmol$_c$/kg in the Ap horizon to 4.37 cmol$_c$/kg in the Btv3 horizon. The low ECEC is indicative of mineralogy dominated by highly weathered clay minerals like kaolinite and iron and aluminum oxides. The XRD analysis confirmed the presence of kaolinite, goethite, quartz, hematite and gibbsite in the clay fraction (< 2 μm) of the soil. A small peak corresponding to 2:1 clay minerals, probably Al-hydroxy interlayer vermiculite or montmorillonite, was observed in clay samples from the Ap, Bt and Btv1 horizons. The major mineral components of the ironstone were goethite, kaolinite and quartz. The fine earth fraction (150 μm) of the Btv1 horizon had a 2.8% CBD extractable iron content and a ratio of OX/CBD less than 0.10, meeting the two requirements established by Soil Taxonomy to qualify as plinthic. The other horizons met the requirement of OX/CBD ratios of less than 0.10, but had less than 2.5% iron extractable by the CBD method. Soil management practices that prevent soil erosion must be implemented in this soil to ward off exposure of plinthite to the surface and its irreversible hardening to ironstone.

Key words: Ultisols, plinthite, ironstone, iron oxides, X ray diffraction

RESUMEN

Propiedades químicas y mineralógicas del suelo Guanajibo arcilloso (Plinthic Kandiudults)

Un perfil del suelo Guanajibo arcilloso (Plinthic Kandiudults) se evaluó para determinar el contenido de petroplintita en los horizontes, la mineralogía y sus propiedades químicas y físicas. Los componentes minerales se determinaron por difracción de rayos x y por técnicas de disolución selectiva, utilizando soluciones de citrato-bicarbonato-ditionato (CBD) y oxalato de amonio (OX). El color del suelo y el de la petroplintita pulverizada se determinó con la carta de colores de Munsell. Además, se evaluó la textura, pH y cationes intercambiables, y la capacidad de intercambio catiónico efectiva (CICE) del suelo. El contenido más alto de petroplintita se observó en el horizonte Ap (4.6%), y disminuyó en los horizontes Bt (0.9%) y Btv1 (1.0%). El contenido de petroplintita aumentó nuevamente en el horizonte Btv2 (3.8%), lo que sugiere que este se formó por depósitos aluviales conteniendo petroplintita. En el horizonte Ap se observó una textura arcillo arenosa y en los demás horizontes, arcillosa, alcanzando el porcentaje mayor de arcilla (92.8%) en el horizonte Btv3, donde no se encontró petroplintita. La CICE fue baja a través de todo el perfil, fluctuando de 2.37 cmol$_c$/kg en el horizonte Ap a 4.37 cmol$_c$/kg en el Btv3. La baja CICE es indicativa de una mineralogía dominada por minerales de arcilla altamente meteorizados, como caolinita y óxidos de hierro y aluminio. El análisis de rayos X (DRX) de la fracción arcillosa confirmó la presencia de caolinita, goetita, cuarzo, hematita y gibsita. Un pico de baja intensidad, correspondiente a minerales 2:1, probablemente vermiculita o montmorilonita interlaminada de hidróxidos de Al, se observó en la arcilla de los horizontes Ap, Bt y Btv1. Los componentes minerales principales observados en la petroplintita fueron goetita, caolinita y cuarzo. La fracción fina del suelo (150 μm) del horizonte Btv1 mostró un contenido de hierro extraíble con CBD de 2.8% y una razón de OX/CBD menor de 0.10, dos requisitos para ser clasificado como plíntico, de acuerdo al sistema de clasificación de Taxonomía de Suelos. En los otros horizontes se observó un contenido de hierro extraíble con CBD menor de 2.5%, pero una razón OX/CBD menor de 0.10. Es necesario implantar prácticas de conservación en este suelo para evitar que la plintita se exponga por erosión a la superficie y que se endurezca irreversiblemente formando petroplintita.

Palabras clave: Ultisols, plintita, petroplintita, óxidos de hierro, difracción de rayos X

INTRODUCTION

Plinthite is an iron-rich, humus-poor mixture of clay with quartz and other highly weathered minerals. It commonly occurs as reddish redox concentrations in a layer that has a polygonal (irregular), platy (lenticular), or reticulated (blocky) pattern. Plinthite irreversibly hardens upon exposure to alternating wetting and drying cycles, especially if exposed to heat from the sun (Eze et al., 2014). Plinthite forms in clay rich subsoils where mineralogy, wetting and drying cycles, temperature, and topography interact to produce the conditions for its formation (Constantine and Priori, 2007; Dos Anjos et al., 1995; Jien and Chen, 2006). Topography influences plinthite formation by affecting the spatial and temporal

distribution of water across landscapes (Eze et al., 2014). Plinthization takes place in soils or horizons that are water saturated for some part of the year. The topographic position is critical for plinthite formation and development, occurring mostly on footslopes and toeslopes where fluctuating moisture conditions prevail (Beauvois, 2009; Jien and Chen, 2006). Heck et al. (1999) indicated that the formation of plinthite and petroplinthite in soils from Brazil was favored by the mobilization of Fe under reducing conditions, followed by oxidation, segregation and aggregation of Fe oxides. These authors also suggested that the eventual transformation of plinthite to petroplinthite involves the transformation of hematite to goethite and dissolution of silicates. Other morphologically similar materials that do not progressively harden upon wetting and drying are not considered plinthite. The horizons in which plinthite occurs commonly have 2.5% (by mass) or more citrate-bicarbonate dithionite (CBD) extractable iron in the fine-earth fraction and a ratio between acid oxalate extractable iron (OX) and CBD extractable iron of less than 0.10 (Soil Survey Staff, 2014).

After irreversible hardening, aggregates are no longer considered plinthite but are regarded as ironstone (Breuning-Madsen et al., 2007). These strongly cemented to indurated ironstone materials can be broken or shattered with a spade but cannot be dispersed even with strong agitation in water with a dispersing agent (Soil Survey Staff, 2014). When plinthite changes irreversibly to ironstone, hardpans or irregular forms of aggregates, plant root growth and soil drainage may be restricted, decreasing soil fertility and exacerbating acidity problems (Eswaran et al., 1990). Intensive soil erosion caused by overgrazing or cropping may bring plinthite to the surface, initiating the hardening process, and thus effectively reduce the soil volume for agricultural and engineering purposes. Even non-cemented, nodular or platy types of plinthite may perch water. In many cases, exposed ironstone disintegrates into hard, gravel-sized fragments that are transported with erosion and mass wasting. When incorporated into younger soils, these fragments reduce the cation exchange capacity (CEC) and total water holding capacity of a soil and may also prove abrasive to agricultural implements (Bigham et al., 2002). Some soils in Southern Australia are so abrasive that conventional tillage points may wear out with as little as four hours of use (Fitzpatrick and Riley, 1990).

In Puerto Rico, plinthite has been recognized in five soil series of the Ultisol and Oxisol orders (Muñoz et al., 2018). These series are Torres (Fine, kaolinitic, isohyperthermic Plinthic Palehumults), Jobos (Fine, kaolinitic, isohyperthermic Plinthaquic Paleudults), Guanajibo (Very-fine, mixed, isohyperthermic Plinthic Kandiudults), Sabana Seca (Very-fine, kaolinitic, isohyperthermic Plinthic Haplaquox) and Almirante (Very-fine

kaolinitic, isohyperthermic Plinthic Hapludox). The quality and agricul-tural potential of these soils can diminish significantly if proper manage-ment to reduce soil erosion and degradation is not implemented.

This study was conducted to evaluate the mineralogy and chemis-try of a Guanajibo soil and the formation and abundance of plinthite and ironstone. Guanajibo soils occupy coastal terraces and alluvial fans. In the past, the major use of this soil was sugarcane production, but at present it is mostly used for pasture and cattle grazing. A seri-ous concern is that overgrazing may exacerbate soil erosion and expose plinthite to an open environment, increasing the formation of iron-stone. Knowledge of the nature of plinthite, its role in reducing water percolation, and its potential to form ironstone and reduce soil quality is necessary to preserve our limited soil resources.

MATERIALS AND METHODS

The research was conducted on a Guanajibo sandy clay (Very-fine, mixed, isohyperthermic Plinthic Kandiudults) located in western Puerto Rico in the municipality of Cabo Rojo (Figure 1). This series consists of very deep, well-drained, moderately permeable soils on terraces and al-luvial fans of humid coastal plains (USDA, 2008). The profile is formed from fine alluvial sediments of mixed origin, deposited on serpentine de-posits (Figure 1). Associated series at the site are Voladora clay (Plinthic Haplohumults) and Delicias clay (Rhodic Hapludox) at higher elevations in the landscape, and Cataño sand (Typic Udipsamments) and Bajura clay (Vertic Endoaquolls) at lower elevations. The typical pedon of the Guanajibo series described by NRCS was selected for the study. The pe-don has five horizons, identified as Ap (0 to 25 cm); Bt (25 to 53 cm); Btv1 (53 to 76 cm); Btv2 (76 to 94 cm) and Btv3 (94 to 160 cm). The soil was described and classified according to USDA Soil Taxonomy, using the Field Book for Describing and Sampling Soils Version 3.0 (USDA, 2012). Soil and ironstone colors were evaluated using Munsell Color Charts.

Soil samples were collected from each horizon, air-dried, ground to pass a 2-mm sieve, and stored in plastic bags for physical and chemi-cal analyses. Particle-size analysis was determined by the centrifuge method (Jackson, 2005) and the separated clay fractions (<2 μm) were saturated with Mg^{2+} and dried using a *Freezone12 Labconco Freeze Dry System*[6]. The clay samples were then ground thoroughly in an agate

[6]Company or trade names in this publication are used only to provide specific infor-mation. Mention of a company or trade name does not constitute an endorsement by the Agricultural Experiment Station of the University of Puerto Rico, nor is this mention a statement of preference over other equipment or materials.
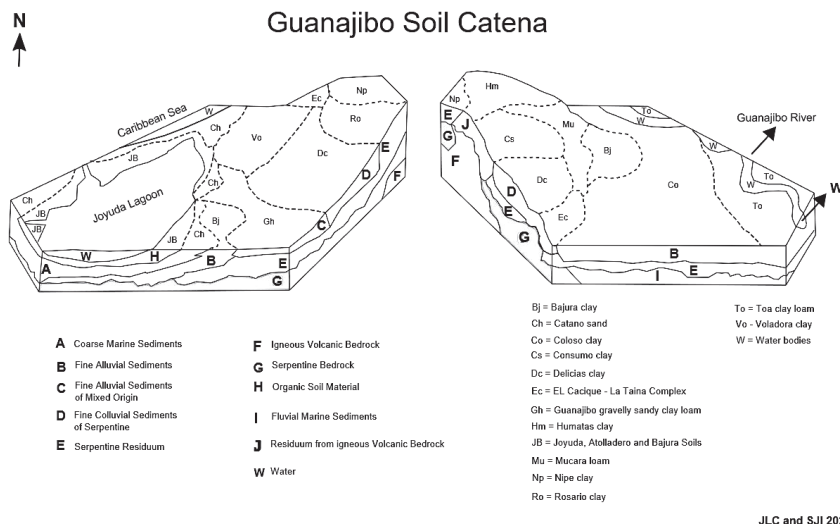
FIGURE 1. Block diagram of Guanajibo soil catena. The authors thank Agro. Jorge L. Lugo-Camacho, Missouri State Soil Scientist, USDA-NRCS, Columbia, Missouri 65203, and Dr. Samuel Indorante, Retired Soil Scientist, USDA-NRCS DuQuain, Illinois 62832, for the preparation of the diagram.

mortar to a fine powder. An X-ray diffraction (XRD) analysis of powdered Mg-clay samples was performed using a *Siemens Diffraktometer D5000* located in the X-Ray Microanalysis Laboratory of the Geology Department at the University of Puerto Rico, Mayagüez. The unit generated Cu Ka radiation and was equipped with a graphite monochromator, computer-controlled theta-compensating slit and an automated sample changer. Step scans were collected from 4 to 70 degrees 2-theta, with two counts per second, at 0.020 degree step intervals. The peaks corresponding to major mineral components were identified.

A 4.5 kg soil sample was used to determine the ironstone content in each horizon. Ironstones were separated from the soil by combined dry and wet sieving, using distilled water. The ironstone particles were thoroughly washed with distilled water and allowed to dry at room temperature. Data on ironstone weight and size were collected. The ironstone weight was recorded and the samples thoroughly ground using an agate mortar, and analyzed by XRD as described previously for the clay samples.

Soil pH was determined in a 1:2 soil:water ratio, using 5.0 g soil samples in 10 ml of distilled water. The samples were agitated for five minutes in a reciprocal shaker, and the pH value measured using an *Orion 960 Autochemistry System*. Exchangeable bases (Ca^{2+}, Mg^{2+} and

K$^+$) were extracted with 1M ammonium acetate buffered at pH 7.0. Exchangeable Al^{3+} was extracted with 1M KCl. All cations were determined by atomic absorption spectroscopy using a *Perkin Elmer AAnalyst 300* (Sumner and Miller, 1996). Effective cation exchange capacity (ECEC) of each soil horizon was determined by the sum of cations.

Free crystalline and "amorphous" iron and aluminum oxide contents were determined by the citrate-bicarbonate dithionite (CBD) (Jackson et al., 1986; Shang and Zelazny, 2008) and the acid ammonium oxalate (OX) methods, respectively (Schwertmann, 1973; Shang and Zelazny, 2008). The CBD solution extracts total free iron oxides (goethite, hematite and maghemite) including amorphous coatings of iron oxides acting as cementing agents in the soil (Shang and Zelazny, 2008). Acid ammonium oxalate selectively dissolves poorly crystalline aluminosilicates, oxides and hydroxides of Al, Fe, Mn and Ti. This treatment can also extract organically bound Fe and Al. The CBD and OX extractions were performed on the fine earth fraction (150 μm) and the ground ironstones. The iron and aluminum extracted were determined by atomic absorption spectroscopy and calculated as a percentage of Fe$_2$O$_3$ and Al$_2$O$_3$.

RESULTS AND DISCUSSION

Soil texture and plinthite occurrence

Soil particle size analyses indicated a clayey texture for all samples, except for the Ap horizon, which was sandy clay. The clay content increased from 39.7% in the Ap horizon to 85.0% in the Bt horizon. The clay content then decreased to 63.8% in the Btv2 but increased again in the Btv3 to 92.7% (Table 1). A sharp increase in clay content in subsurface horizons is a distinguishing characteristic of Ultisols due to clay illuviation and/or in situ clay formation (Simonson, 1949; Miller, 1993); however, the Guanajibo soil is an Ultisol formed from fine-grained sediments of mixed origin, so variations in clay content may also reflect changes in parent material stratigraphy. The Ap and the Btv2 horizons showed the largest content of sand, 50.4 and 31.2%, respectively. These

TABLE 1.—*Soil horizons depth and textural analysis.*

Horizon	Depth (cm)	% Sand	% Silt	% Clay	Texture
Ap	0 - 25	50.4	9.9	39.7	Sandy clay
Bt	25 - 53	11.0	4.0	85.0	Clay
Btv1	53 - 76	13.9	9.4	76.7	Clay
Btv2	76 - 94	31.2	5.0	63.8	Clay
Btv3	94 - 160	6.2	1.1	92.7	Clay

two horizons also showed the largest content of ironstone fragments (Table 2), an indication that the decomposition of ironstone is contributing to the sand content of these two horizons.

Plinthite originates through an accumulation process that involves extreme weathering and selective removal of other constituents (Bigham et al., 2002). Platy and irregular bodies of plinthite predominate in the Btv horizons and increase in abundance with depth on a volumetric basis. Strong brown and reddish coloration were predominant in these horizons (Table 3). Color is probably the most widely used but most inconsistent soil property when identifying plinthite. Plinthite identification by color alone will most likely lead to many discrepancies because color is due to both the type and relative amount of iron oxides (Daugherty and Arnold, 1982). The USDA-Natural Resources Conservation Service (NRCS) reports that plinthite chromas are usually 6 or less, whereas the chromas of non-plinthite are greater than 6. The hues determined in this study mostly ranged from 7.5YR to 2.5YR throughout the Guanajibo soil profile; however, 2.5Y and 10YR colors were observed in the Btv3 horizon (Table 3), which presented the greatest amount of color variations. The hue of the ironstone was 7.5YR throughout the soil profile. Daniels et al. (1978) reported hues ranging from 10 R to 7.5YR, with a strong prevalence of 5YR hue. Eswaran and Mohan (1973) found goethite was most frequently associated with soils having color in the range of 2.5Y to 7.5YR and hematite commonly associated with hues of 10R to 5YR.

Ironstone quantification

The greatest amount and size of ironstone were observed in the Ap horizon, with 205 g of ironstone per 4.5 kg of soil (Table 2). The Btv2 horizon contained the second greatest amount of ironstone with 172 g per 4.5 kg of soil. These horizons also had the greatest amount of sand, probably because of mechanical degradation of ironstone. The Guanajibo soil is formed from alluvial deposits, and the higher amount of ironstone in the Btv2 horizon, compared with the Btv1 and Bt horizons

TABLE 2.—*Ironstone content in Guanajibo soil horizons.*

Horizon	Depth (cm)	Weight (g)*	% Ironstone
Ap	0 - 25	205	4.6
Bt	25 - 53	41	0.9
Btv1	53 - 76	45	1.0
Btv2	76 - 94	172	3.8
Btv3	94 - 160	0	0

*Grams of ironstone in a 4.5 kg soil sample.

Table 3.—*Soil color and ground ironstone color in Guanajibo horizons.*

Horizon	Soil Munsell Designation	Soil Color	Ironstone Munsell Designation	Soil Color
Ap	5 YR 3/2	Dark reddish brown	7.5 YR 4/6	Strong brown
Bt	7.5 YR 5/8	Strong brown	7.5 YR 5/8	Strong brown
Btv1	7.5 YR 5/6	Strong brown	7.5 YR 4/4	Brown
	2.5 YR 4/8	Red		
Btv2	7.5 YR 5/6	Strong brown	7.5 YR 5/8	Strong brown
	2.5 YR 4/6	Red		
Btv3	2.5 Y 5/6	Light olive brown	None	
	2.5 Y 8/3	Pale brown		
	2.5 YR 3/6	Dark red		
	7.5 YR 4/6	Strong brown		
	10 YR 4/3	Brown		

suggests the occurrence of different events of material deposition. The Btv2 horizon was probably once a surface layer exposed to induration or accumulation of ironstone fragments from higher elevations in the landscape. Subsequent deposition and weathering processes formed the Ap, Bt and Btv1 horizons in the modern Guanajibo soil. Ironstone is completely absent in the Btv3 horizon, where plinthite is more prominent but has not been exposed to aeration and the drying cycles that cause irreversible induration.

pH, exchangeable Al^{3+}, exchangeable basic cations and ECEC

The pH values of the Guanajibo pedon ranged from 4.3 to 4.7 (Table 4). These values were classified as strongly acidic throughout the soil profile. The pH values of the Ap and Bt horizons were similar and the lowest, 4.4 and 4.3, respectively. These two horizons also showed the highest content of exchangeable Al^{3+}. Exchangeable Al^{3+} decreased in the deeper Btv2 and Btv3 horizons, where slightly higher pH values were observed.

Table 4.—*pH, exchangeable cations and effective cation exchange capacity of Guanajibo soil horizons.*

Horizon	pH	K$^+$	Ca^{2+}	Mg^{2+}	Na$^+$	Al^{3+}	ECEC
		------------------- cmol$_c$/kg -------------------					
Ap	4.4	0.10	0.71	0.55	0.04	0.97	2.37
Bt	4.3	0.02	1.87	0.74	0.20	0.50	3.33
Btv1	4.4	0.02	2.51	0.74	0.23	0.09	3.59
Btv2	4.7	0.01	1.97	0.55	0.19	0.07	2.79
Btv3	4.6	0.01	3.16	0.95	0.23	0.02	4.37

The ECEC of the soil is dependent on the amount and type of clay minerals and organic matter. Low values of ECEC in soils are attributed to low organic matter content and the presence of clay minerals with low CEC, such as kaolinite, and the oxides of Fe and Al. Higher ECEC values (>25 cmol$_c$/kg) indicate the presence of hydrous micas, chlorite, and interstratified clay minerals (Odell et al., 1974). The ECEC of the Guanajibo soil was low (2.4 to 4.4 cmol$_c$/kg) throughout (Table 4), indicating the presence of weathered clays, such as oxides and kaolinite, with low ECEC values in the range of 3 to 15 cmol$_c$/kg. The ECEC measured was greatest in the Btv3 horizon, which also had the highest clay content.

Free iron and aluminum oxide content

Soil samples were ground to pass a #100 (150 μm) mesh sieve. The content of total "free iron" was determined by the citrate bicarbonate dithionite (CBD) extraction. For the poorly crystalline components, an ammonium oxalate (OX) (pH 3.0) extraction was performed. Data on iron and aluminum percentages for each horizon of the Guanajibo soil profile are shown in Table 5. The ratios between ammonium oxalate and citrate bicarbonate dithionite (OX/CBD) extractable iron, and aluminum are also included. The active iron ratio indicates the relative proportion of non crystalline to crystalline iron. A low value indicates a high tendency for plinthite formation, since plinthite needs a high proportion of crystalline iron to harden. This measurement has been used as an indicator of the presence of plinthite (Daugherty and Arnold, 1982). According to the Soil Survey Staff (1999), a plinthic horizon must have a OX/CBD Fe ratio of less than 0.10. All horizons in the Guanajibo soil profile fulfill this requirement (Table 5). Poorly crystalline iron oxides generally comprise a small percentage of the total oxide content in Ultisols (Gamble and Daniels, 1972).

TABLE 5.—*Iron and aluminum extracted from Guanajibo soil using CBD and Oxalate solutions.*

Soil Horizon	Iron				Aluminum			
	% OX	% CBD	% Fe$_2$O$_3$	Ratio OX/CBD	% OX	% CBD	% Al$_2$O$_3$	Ratio OX/CBD
Ap	0.03	1.12	1.60	0.03	0.30	0.43	0.80	0.70
Bt	0.03	1.17	2.43	0.03	0.25	0.60	1.14	0.42
Btv1	0.02	2.82	4.03	0.01	0.31	0.80	1.50	0.39
Btv2	0.03	1.90	2.72	0.02	0.39	0.34	0.63	1.15
Btv3	0.02	2.14	3.06	0.01	0.49	0.25	0.47	1.96

The active iron ratios are generally higher in surface soils than in the subsoil (Gamble and Daniels, 1972); however, the Btv2 horizon had an active ratio almost as high as that of the Ap horizon. This observation adds to our theory that the Btv2 horizon was a surface layer at some time, during the pedological process of soil formation.

Another requirement for a plinthic horizon is that the CBD extractable Fe in the fine soil fraction must be at least 2.5%. In our study only the Btv1 meets this requirement, containing 2.82% of CBD extractable Fe. The CBD extractable Fe of the Btv2 and Btv3 horizons were 1.90% and 2.14%, less than Btv1 and less than the USDA-NRCS requirement of 2.5% of CBD extractable Fe. However, the OX/CBD Fe ratio of less than 0.10 was fulfilled. The higher percentage of CBD extractable Al was observed in the Bt (0.60) and in the Btv1 (0.80) horizons. The CBD extractable Al decreased in the lower Btv2 and Btv3 horizons, and the amorphous OX extractable Al increased (Table 5). The presence of silicate minerals, like low crystallinity kaolinite also contributes to the increase in OX extractable Al in the lower horizons (McKeague and Day, 1966). On the other hand, CBD extractable Fe increased in these horizons compared with the Ap and Bt horizons. The data indicates an increase in crystallinity of iron oxides in the plinthic horizons and a decrease in crystallinity of aluminum oxides.

The CBD and OX extractions were also performed on the ironstone fragments from each horizon, using a fine earth fraction (150 µm) (Table 6). "Free" iron or crystalline iron extracted by the CBD method ranged from 2.0 to 2.5%. For aluminum it ranged from 0.82 to 1.30%. Ironstone pebbles had lower OX/CBD ratios for iron and aluminum than the soil fines, indicating the presence of more crystalline oxides. The pedological processes leading to ironstone formation seem to increase the crystallinity of both oxidic fractions. Similar results were reported by Coelho and Vidal-Torrado (2003) in soils from Brazil.

TABLE 6.—*Iron and aluminum extracted from ironstone in Guanajibo soil using CBD and Oxalate solutions.*

	Iron				Aluminum			
*Soil Horizon	% OX	% CBD	% Fe_2O_3	Ratio OX/CBD	% OX	% CBD	% Al_2O_3	Ratio OX/CBD
Ap	0.04	2.10	3.06	0.02	0.01	0.82	1.56	0.01
Bt	0.03	2.00	2.86	0.01	0.02	1.13	2.13	0.02
Btv1	0.03	2.10	3.04	0.01	0.02	1.30	2.46	0.02
Btv2	0.03	2.50	3.53	0.01	0.02	1.29	2.43	0.02

*No ironstone fragments were found in the Btv3 horizon.

X-ray diffraction analysis

The X-ray diffraction analysis indicated the presence of gibbsite, goethite, kaolinite, quartz and hematite as major mineral components in the clay fraction and in the ironstone (Figures 2 to 10). The intense peaks of goethite are indicative of its predominance in these highly weathered soils where goethite is commonly associated with lesser quantities of hematite, maghemite and magnetite (Schwertmann and Taylor, 1977; Gamble and Daniels, 1972). The most intense peaks for kaolinite (12.2 degrees 2 theta), gibbsite (17.0 degrees 2 theta) and goethite (21.5 degree 2 theta) were used to estimate the intensity ratios from each diffractogram (Table 7). The predominance of kaolinite over gibbsite is clear in the intensity ratio values ranging from 9 to 13 (Table 7). Higher ratios of K/Gb were observed in the Ap and the Btv3 horizons. Gibbsite formation can be inhibited in the surface Ap horizon by the presence of organic acids. The organic anions in soils vary in molecular weight, structure and number of functional groups. Some organic acids like citric, tartaric, oxalic and fulvic interfere with the crystallization of $Al(OH)_3$ and facilitate the movement of aluminum compounds through the soil profile to lower horizons (Violante and Huang, 1985). Also, a small XRD peak corresponding to 2:1 clays was observed in the Ap horizon, probably chlorite or hydroxy interlayered vermiculite and montmorillonite (Figure 2). These clay minerals caused what
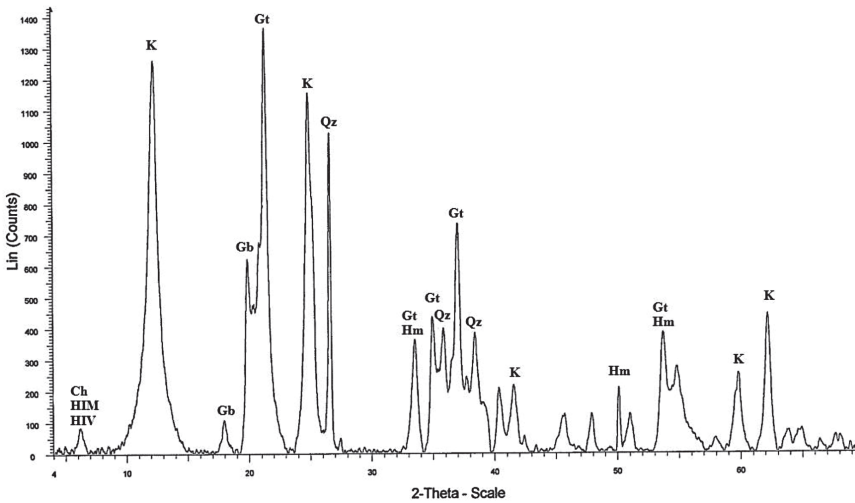

FIGURE 2. X-ray diffraction pattern of the clay fraction extracted from the Ap horizon (0 to 25 cm) of Guanajibo soil. (Ch) chlorite, (HIV) hydroxy interlayer vermiculite, (HIM) hydroxy interlayer montmorillonite, (Gt) goethite, (K) kaolinite, (Qz) quartz, (Hm) hematite, (Gb) gibbsite
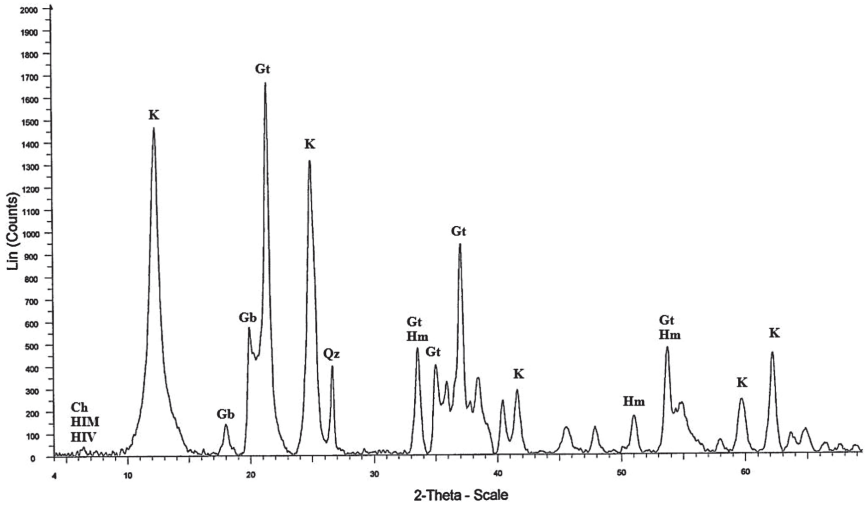
Figure 3. X-ray diffraction pattern of the clay fraction extracted from the Bt horizon (25 to 53 cm) of Guanajibo soil. (Ch) chlorite, (HIV) hydroxy interlayer vermiculite, (HIM) hydroxy interlayer montmorillonite, (Gt) goethite, (K) kaolinite, (Qz) quartz, (Hm) hematite, (Gb) gibbsite

has been called the anti-gibbsite effect, the formation of interlayers of aluminum hydroxide between the 2:1 layers thereby reducing the formation of gibbsite (Jackson, 1962). Kaolinite will also inhibit gibbsite
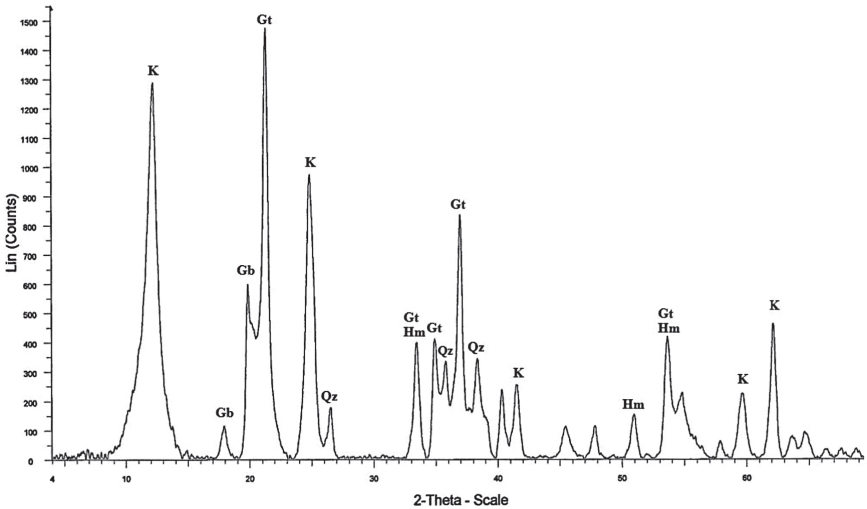

Figure 4. X-ray diffraction pattern of the clay fraction extracted from the Btv1 horizon (53 to 76 cm) of Guanajibo soil. (Gt) goethite, (K) kaolinite, (Qz) quartz, (Hm) hematite, (Gb) gibbsite
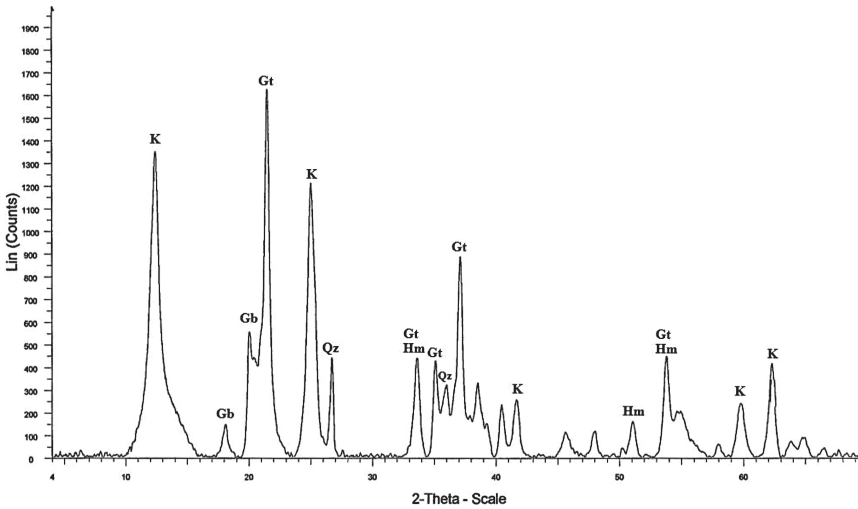
FIGURE 5. X-ray diffraction pattern of the clay fraction extracted from the Btv2 horizon (76 to 94 cm) of Guanajibo soil. (Gt) goethite, (K) kaolinite, (Qz) quartz, (Hm) hematite, (Gb) gibbsite

formation due to the incorporation of Al^{3+} in the kaolinite structure, a mechanism that may be occurring in the Btv3 horizon. The formation in situ of kaolinite in the Btv3 horizon suggests silica movement
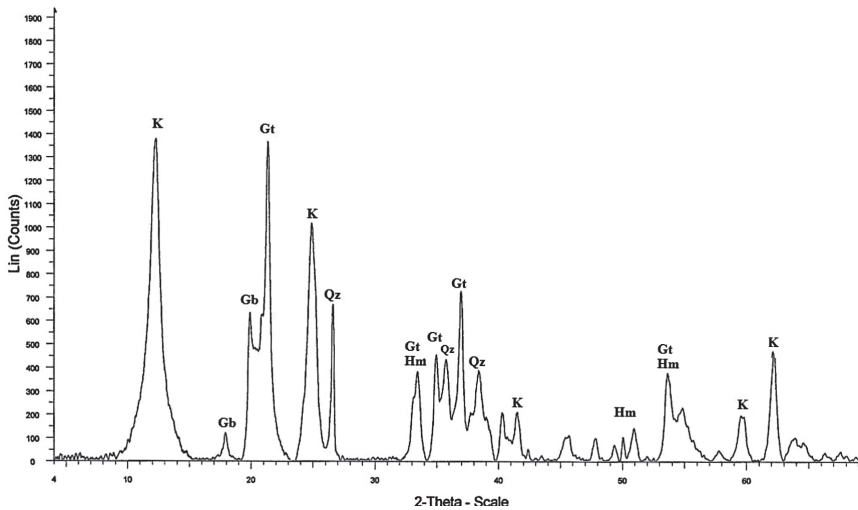

FIGURE 6. X-ray diffraction pattern of the clay fraction extracted from the Btv3 horizon (94 to 160 cm) of Guanajibo soil. (Gt) goethite, (K) kaolinite, (Qz) quartz, (Hm) hematite, (Gb) gibbsite
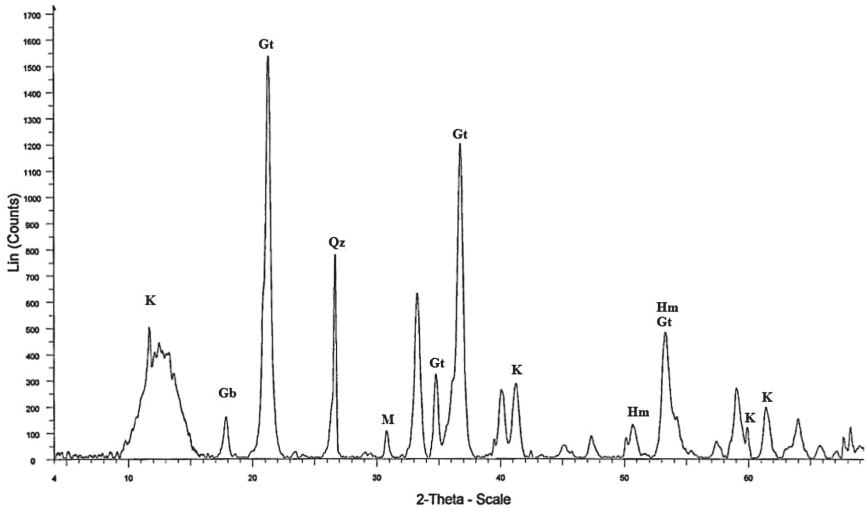
FIGURE 7. X-ray diffraction pattern of ground ironstone from the Ap horizon (0 to 25 cm) of Guanajibo soil. (Gt) goethite, (K) kaolinite, (Qz) quartz, (Hm) hematite, (Gb) gibbsite, (M) magnetite

through the soil profile. The predominance of goethite over kaolinite is evident by the low K/Gt ratios of 1.0 or less. Larger intensity peaks for goethite are observed in the middle horizons.
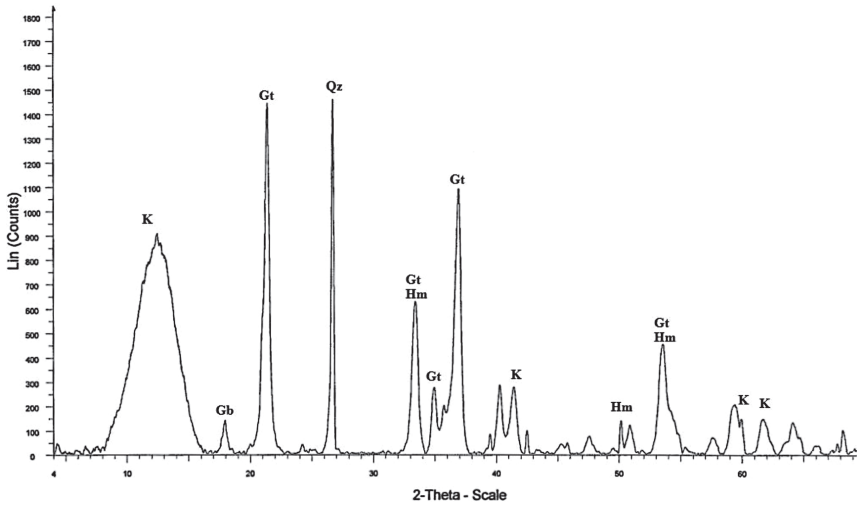
FIGURE 8. X-ray diffraction pattern of ground ironstone from the Bt horizon (25 to 53 cm) of Guanajibo soil. (Gt) goethite, (K) kaolinite, (Qz) quartz, (Hm) hematite, (Gb) gibbsite
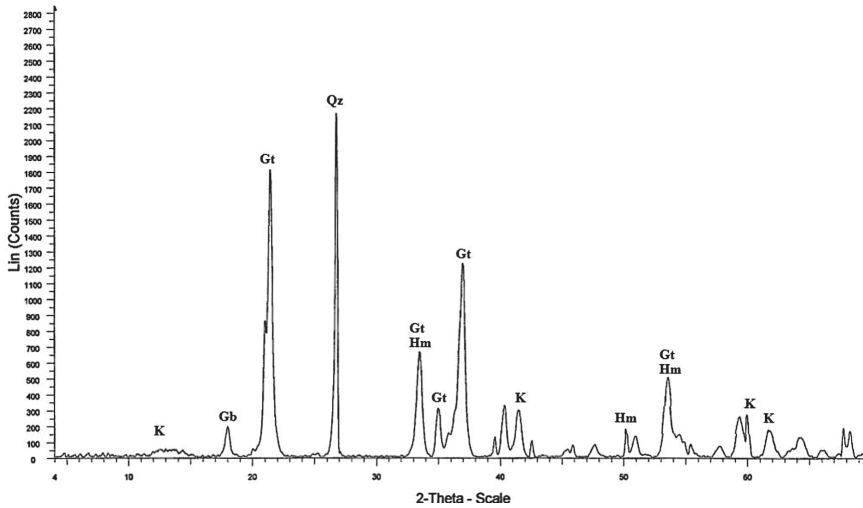
FIGURE 9. X-ray diffraction pattern of ground ironstone from the Btv1 horizon (53 to 76 cm) of Guanajibo soil. (Gt) goethite, (K) kaolinite, (Qz) quartz, (Hm) hematite, (Gb) gibbsite

The predominance of oxides and kaolinite in the clay fractions of the Guanajibo soil agrees with the low ECEC observed throughout the profile (Table 4). A small peak corresponding to 2:1 clays,
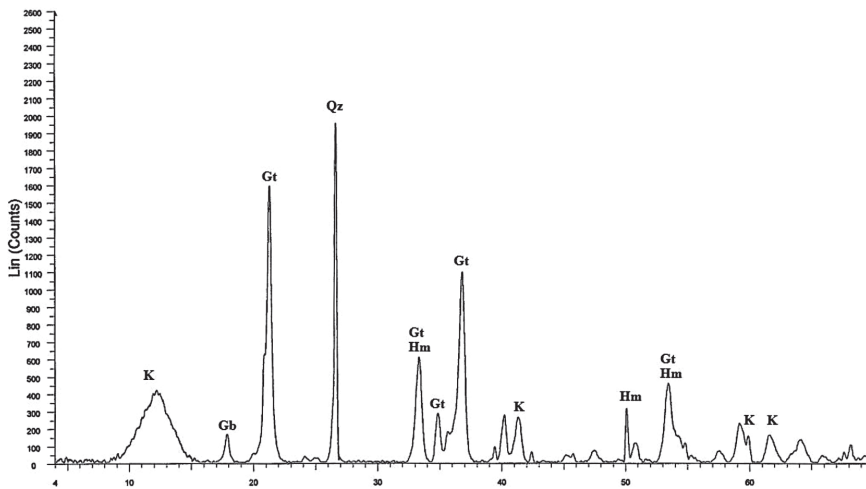

FIGURE 10. X-ray diffraction pattern of ground ironstone from the Btv2 horizon (76 to 94 cm) of Guanajibo soil. (Gt) goethite, (K) kaolinite, (Qz) quartz, (Hm) hematite, (Gb) gibbsite

TABLE 7.—*XRD peak intensity ratio for kaolinite/gibbsite, kaolinite/goethite and goethite/gibbsite in clay fraction and ironstone.*

Horizon	Clay fraction					
	K Intensity	Gb Intensity	Gt Intensity	K/Gb	K/Gt	Gt/Gb
Ap	1280	100	1390	12.8	0.9	13.9
Bt	1475	150	1700	9.8	0.9	11.3
Btv1	1300	125	1480	10.4	0.9	11.8
Btv2	1350	150	1675	9.0	0.8	11.2
Btv3	1390	100	1375	13.8	1.0	13.8
	Ironstone					
Ap	450	150	1550	3.0	0.29	10.3
Bt	900	150	1450	6.0	0.62	9.7
Btvl	50	175	1825	0.3	0.03	10.4
Btv2	400	150	1600	2.7	0.25	10.7

probably hydroxy interlayered vermiculite or montmorillonite, was observed at 6.2 degrees 2 theta in the clay samples of Ap, Bt and Btv1 horizons (Figures 2 to 4). The intensity of this peak decreased with soil depth, and it is not observed in the Btv2 and Btv3 horizons. Kaolinite, and iron and aluminum oxides predominate in the mineralogy of Ultisols, but Al-hydroxy interlayered vermiculite and smectites can form during the weathering process and are usually present in lesser quantities in the profile (Miller, 1983; Lynn et al., 2002).

The kaolinite peaks in the ironstone were broader and of lower intensity, probably the result of poor grinding of the samples, and/or lower crystallinity. However, intense and sharp peaks of goethite and quartz were observed. Peaks corresponding to gibbsite and hematite were of lower intensity, as was the case for the clay fraction. A small, well-defined peak corresponding to magnetite and or maghemite was observed in the ironstone from the Ap horizon at 31 degrees 2 theta (Figure 7). Such peaks were not observed in the ironstone samples from other horizons. The fact that this peak is only observed in the surface Ap horizon suggests that maghemite may have formed as result of burning of other oxides like goethite. Transformation of goethite to maghemite as a result of pasture burning has been reported under field and laboratory conditions (Grogan et al., 2003; Nornberg et al., 2004). The farm where this study was conducted is under pasture, and fires are common during the dry season. A broad kaolinite peak of low intensity was observed in the ironstone from the Btv1 horizon, indicative of lower concentrations of this clay mineral. The K/Gt and K/Gb intensity

peak ratios were very low in the ironstone when compared to the ratios observed for the clay fraction. This finding suggests loss of kaolinite during the transformation process of plinthite to ironstone, resulting in a relative enrichment of iron and aluminum oxides.

CONCLUSIONS

Soil color and color patterns are the first criteria used to identify plinthite under field conditions. Platty and irregular bodies of plinthite were observed in the Guanajibo soil profile from 53- to 160-cm depth. Dark brown and reddish coloration were predominant in these horizons. Sand content was related to the quantity of ironstone; horizons with higher amounts of ironstone also showed a higher amount of sand. An increase in ironstone was observed in the Btv2 horizon, which supported the alluvial formation of this soil. The ECEC was lower in the Ap horizon and increased in the Bt horizons with increasing clay content. A decrease in ECEC was observed in the Btv2 horizon where the ironstone and sand content increased. The opposite was observed in the Btv3 horizon, which contained higher clay and the lowest sand content among all horizons. Exchangeable Al^{3+} was higher in the upper horizons, contributing to the acidity of the soil. The amounts of CBD extractable Fe were less than expected. Only the Btv1 horizon fulfilled the requirements and characteristics to be classified as plinthic, as described by USDA-NRCS. The Btv2 and Btv3 did not have the minimum CBD extractable iron content to be called plinthic; however, the Btv1, Btv2 and Btv3 fulfill the requirement of an OX/CBD ratio less than 0.10. Ironstone pebbles had lower OX/CBD ratios than soil fines, indicating the presence of more crystalline iron oxides in the ironstone.

The XRD analysis indicated that goethite, kaolinite, quartz, hematite and gibbsite were the principal mineral components in the clay fractions in all horizons. A low intensity peak attributed to Al hydroxy interlayered vermiculite or montmorillonite was clearly observed in the Ap, Bt and Btv1 clay fractions, but decreased in intensity and was barely detected in the Btv2 and Btv3 horizons. In the ironstone samples, goethite and quartz peaks were the most intense.

Soil conservation practices must be implemented in these soils to prevent the exposure of plinthite to the surface and subsequent formation of ironstone. Soil management practices with minimum soil disturbance, such as minimum-till or no-till, are recommended to prevent soil loss and erosion.

LITERATURE CITED

Beauvais, A., 2009. Ferricrete biochemical degradation on the rainforest-savannas boundary of Central African Republic. *Geoderma* 150: 379-388.

Bigham, J.M., R.W. Fitzpatrick and D.G. Schulze, 2002. Iron oxides: pp 323-366, *In*: J.B. Dixon and D. Schulze (eds.) Soil Mineralogy with Environmental Applications. SSSA Book ser. 7. SSSA, Madison, WI.

Breuning-Madsen, H., T.W. Awadzi, C.B. Koch and O.K. Borggard, 2007. Characterization and genesis of pisolitic soil layers in a tropical moist semi-deciduous forest of Ghana. *Geoderma* 141: 130-138.

Coelho, M.R. and P. Vidal-Torrado, 2003. Characterization and genesis of plinthic profiles developed from sandstone (Bauru Group). II. Mineralogical properties. *Rev. Bras. Cienc. Solo* 27: 495-507.

Constantine, E.A.C. and S. Priori, 2007. Pedogenesis of plinthite during early Pliocene in the Mediterranean environment: Case study of buried Paleosol at Podere Renieri, central Italy. *Catena* 71: 425-443.

Daniels, R.B., H.F. Perkins, B.F. Hajek and E.E. Gamble, 1978. Morphology of discontinuous phase plinthite and criteria for its field identification in the southeastern United States. *Soil Sci. Soc. Am. J.* 42: 944-949.

Daugherty, L.A. and R.W. Arnold, 1982. Mineralogy and iron characterization of plinthic soil on alluvial landforms in Venezuela. *Soil Sci. Soc. Am. J.* 46: 1244-1252.

Dos Anjos, L.H.C., D.P. Franzmeier and D.G. Schulze, 1995. Formation of soils with plinthite on a toposequence in Maranhao state, Brazil. *Geoderma* 64: 257-279.

Eswaran, H. and N.G.R. Mohan, 1973. The microfabric of petroplinthite. *Soil Sci. Soc. Am.* 37: 79-82.

Eswaran, H., F. De Coninck and T. Varghese, 1990. Role of plinthite and related forms in soil degradation: pp 109-127, *In*: R. Lal and B. A. Stewart (eds) Advances in Soil Science. Springer Verlag New York, USA.

Eze, P.N., T.K. Udeigwe and M.E. Meadows, 2014. Plinthite and its associated evolutionary forms in soils and landscapes: A review. *Pedosphere* 24(2): 153-166.

Fitzpatrick, R.C. and T.W. Riley, 1990. Abrasive soils in Australia: Mineralogical Properties and classification. 14th International Soil Science Society Conference, Kyoto, Japan. Vol. VII: 404-405.

Gamble, E.E. and R.B. Daniels, 1972. Iron and silica in water, acid ammonium oxalate and dithionate extracts of some North Carolina coastal plain soils. *Soil Sci. Soc. Am. Proc.* 36: 939-943.

Grogan, K., R.J. Gilkes and B.G. Lotterman, 2003. Maghemite formation in burnt plant litter at East Trinity, North Queensland, Australia. *Clays and Clay Minerals* 51(4): 390-396.

Heck, R.J., A.R. Mermut and M.C. Santos, 1999. Iron oxides in plinthic soils on sedimentary deposits in northeastern Brazil. *Rev. Bras. Cienc. Solo* 23: 651-660.

Jackson, M.L., 1962. Interlayering of expansible layer silicates in soils by chemical weathering. *Clay and Clay Miner*. 11: 29-46.

Jackson, M.L., 2005. Soil Chemical Analysis–Advanced Course. IW-Madison Libraries. Parallel Press. 930 pp.

Jackson, M.L., C.H. Lim and L.W. Zalazny, 1986. Oxides, hydroxides and aluminosilicates: pp 101-150, *In*: A. Klute (ed) Methods of Soil Analysis. Part I. 2nd ed. Agron. Monogr. 9. ASA and SSSA. Madison, WI.

Jien, S.H. and Z.S. Chen, 2006. Characterization and formation of iron-manganese nodules of Ultisols with plinthite in Taiwan. *In*: Proceedings of the 18th World Congress of Soil Science. July 9-15. 2006. Philadelphia, PA.

Lynn, W.C., R.J. Ahrens and A.L. Smith, 2002. Soil minerals, their geographic distribution and soil taxonomy: pp 691-709, *In*: J. B. Dixon and D. G. Schulze (eds) Soil Mineralogy with Environmental Applications. SSSA Book Series, no 7. Soil Sci. Soc. Am., Madison, WI.

McKeague, J.A. and J.H. Day, 1966. Dithionite and oxalate- extractable Fe and Al as aids in differentiating various classes of soils. *Can. J. Soil Sci.* 46: 13-22.

Miller, B.J., 1983. Ultisols: pp 283-323, *In*: L.P. Wilding, N.E. Smeck and G.F. Hall (eds) Pedogenesis and Soil Taxonomy. II. The Soil Orders, Elsevier Science Publishers B.V., Amsterdam, Netherlands. 410 pp.

Muñoz, M.A., W.I. Lugo, C. Santiago, M. Matos, S. Ríos and J. Lugo, 2018. Taxonomic classification of the soils of Puerto Rico, 2017. Agric. Expt. Station, Univ. P. R. Bulletin 313. 73 pp.

Nornberg, P., U. Schwertmann, H. Stanjek, T. Andersen and H.P. Gunnlaugsson, 2004. Mineralogy of a burned soil compared with four anomalously red quaternary deposits in Denmark. *Clay Minerals* 39: 85-98.

Odell, R.T., J.C. Dijkerman, W. van Vuure, S.W. Melsted, A.H. Beavers and P.M. Sutton, 1974. Characteristics, classification and adaptation of soils in selected areas in Sierra Leone, West Africa. Department of Agronomy, Njala University, Sierra Leone, Bull. 4 and Univ. of Illinois, 748.

Schwertmann, U., 1973. Use of oxalate for Fe extraction from soils. *Can. J. Soil Sci.* 53: 244-246.

Schwertmann, U. and R.M. Taylor, 1977. Iron oxides: pp 145-180, *In*: J.B. Dixon and S. B. Weed (eds) Minerals in the Soil Environments. Soil Science Soc. America, Madison, WI.

Shang, C. and L.W. Zelazny, 2008. Selective dissolution techniques for mineral analysis of soils and sediments: pp 33-80. *In*: A. L Ulery and L. Richard Drees (eds) Methods of Soil Analysis, Part 5. Mineralogical Methods. SSSA Book Series, no. 5, Soil Science Society of America, Madison, WI, 521 pp.

Simonson, R.W., 1949. Genesis and classification of Red Yellow Podzolic soils. *Soil Sci. Soc. Am. Proc.* 14: 316-319.

Soil Survey Staff, 2014. Keys to Soil Taxonomy. Twelfth Edition, Natural Resources Conservation Service, U.S. Department of Agriculture, 360 pp.

Soil Survey Staff, 1999. Soil Taxonomy: A Basic System of Soil Classification for Making and Interpreting Soil Surveys. 2th ed. Natural Resources Conservation Service, U.S. Department of Agriculture.

Sumner, M.E. and W.P. Miller, 1996. Cation exchange capacity and exchange coefficients: pp 1201-1230, *In*: Sparks et al. (eds) Methods of Soil Analysis. Soil Science Society of America. Madison, WI, 1390 pp.

United States Department of Agriculture, Natural Resources Conservation Service, 2008. Soil Survey of San Germán Area, Puerto Rico. Accessible online at: http://soils.usda.gov/survey/printed_surveys/.

United States Department of Agriculture, Natural Resources Conservation Service, 2012. Field Book for Describing and Sampling Soils, Version 3.0. National Soil Survey Center.

Violante, A. and P. M. Huang, 1985. Influence of inorganic and organic ligands on the formation of aluminum hidroxides and oxyhydroxides. *Clays Clay Miner*. 33: 181-192.